analytical chemistry

Article

pubs.acs.org/ac

Selection and Identification of DNA Aptamers against Okadaic Acid for Biosensing Application

Shimaa Eissa,[†] Andy Ng,[‡] Mohamed Siaj,[§] Ana C. Tavares,[†] and Mohammed Zourob*[,‡]

[†]Institut National de la Recherche Scientifique, Centre—Énergie, Matériaux et Télécommunications, 1650 Boulevard Lionel Boulet, Varennes, Québec J3X 1S2, Canada

[‡]Center of Biomedical Engineering, School of Engineering, Cranfield University, Cranfield, Bedfordshire MK43 0AL, United Kingdom

[§]Département de Chimie et Biochimie, Université du Québec à Montréal, Montréal, Québec H3C 3P8, Canada

Supporting Information

ABSTRACT: This work describes the selection and identification of DNA aptamers that bind with high affinity and specificity to okadaic acid (OA), a lipophilic marine biotoxin that accumulates in shellfish. The aptamers selected using systematic evolution of ligands by exponential enrichment (SELEX) exhibited dissociation constants in the nanomolar range. The aptamer with the highest affinity was then used for the fabrication of a label-free electrochemical biosensor for okadaic acid detection. The aptamer was first immobilized on the gold electrode by a self-assembly approach through Au−S interaction. The binding of okadaic acid to the aptamer immobilized on the electrode surface induces an alteration of the aptamer conformation causing a significant decrease in the electron-transfer resistance monitored by electrochemical impedance spectroscopy. The aptasensor showed a linear range for the concentrations of OA between 100 pg/mL and 60 ng/mL with a detection limit of 70 pg/mL. The dissociation constant of okadaic acid with the aptamer immobilized on the electrode surface showed good agreement with that determined using fluorescence assay in solution. Moreover, the aptasensor did not show cross-reactivity toward toxins with structures similar to okadaic acid such as dinophysis toxin-1 and 2 (DTX-1, DTX-2). Further biosensing applications of the selected aptamers are expected to offer promising alternatives to the traditional analytical and immunological methods for OA detection.

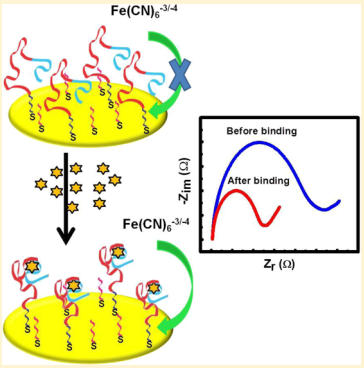

Okadaic acid (OA) is a lipophilic, heat-stable phycotoxin produced by algae of the genera Dinophysis and Prorocentrum.[1] OA has several analogues, such as the dinophysis toxins (DTX1, DTX2) (Supporting Information Figure S1), which have very similar structures, but not all of them have the same toxicity levels. OA accumulates in various species of shellfish, mainly in mussels, scallops, oysters, and clams. The ingestion of OA-contaminated shellfish by human causes diarrheic shellfish poisoning characterized by symptoms such as abdominal pain, nausea, vomiting, and diarrhea.[2] The toxicity of OA is assumed to be due to the inhibition of protein phosphatases, PP1 and PP2A enzymes.[3,4] Moreover, OA has shown tumor promotion and immunotoxic effects.[5] Since the contamination of shellfish with OA has harmful impact on the human health as well as shellfish industry worldwide, detection methods for OA are being developed. The mouse bioassay[6] was the reference method recommended by the European Commission (EC) for the detection of OA until 2011. However, its lack of sensitivity, selectivity, and ethical concerns led the EC to recommend alternative methods[7] such as chromatography coupled to fluorescence or mass spectrometry, protein phosphatase inhibition assays or immunoassays, particularly enzyme-linked immunosorbent assay (ELISA). However, there is still an urgent need to develop new detection methods which can perform rapid, simple, cost-effective, and sensitive monitoring of OA in shellfish. Immunosensors have recently been shown as emerging screening tools for many target analytes, including OA. Much research work has been devoted to develop immunosensors for OA using different transducers such as chemiluminescence,[8] surface plasma resonance,[9] piezoelectric,[10] quartz crystal microbalance,[11] and electrochemical detection.[7,12,13] Electrochemical immunosensors are more favorable due to the lower cost of the equipment and the possibility of miniaturization. However, most of the developed immunosensors for OA were based on indirect competitive assays,[7,12,13] which require the use of two antibodies, enzyme and reporter reagents, in addition to a number of incubations and washing steps. Recently, we developed a sensitive immunosensor for OA based on direct competitive assay which enables single-step detection without the need of enzyme labeling.[14] Nevertheless, the high cost of the antibodies, the limited stability, and required special storage conditions are still challenges facing immunosensor technologies these days.

Received: July 19, 2013
Accepted: October 29, 2013

   dx.doi.org/10.1021/ac402220k | *Anal. Chem.* XXXX, XXX, XXX−XXX

Aptamers are short synthetic oligonucleotides selected from combinatorial libraries of random sequences by in vitro selection which have been appeared as an excellent alternative to antibodies. Since the selection of the first aptamers in 1990,[15,16] many aptamers have been isolated so far with high affinity and specificity to a wide range of target analytes including proteins, peptides, cells, and small molecules.[17] Aptamers as recognition receptors have several advantages over antibodies: (1) they can be prepared by in vitro selection procedure without using experimental animals, (2) can be developed even against toxins or low molecular weight compounds which is hardly achievable with antibodies, (3) can be readily synthesized with very low cost, (4) their facile chemical modification by various chemical tags allows the immobilization of aptamers onto various solid supports, (5) they are highly stable in different conditions which allows the long-term storage and the transportation at ambient temperature, unlike the antibodies which can undergo irreversible denaturation, and (6) their conformational change upon binding with the target can be exploited in designing direct detection strategies of the target analytes. Due to these advantages, aptamers as recognition receptors are emerging as novel capturing agents that could replace antibodies in biosensor applications.[18] Until now, few aptamers targeting toxins such as ochratoxin A,[19] fumonisin B1,[20] and saxitoxin[21] have been selected. For okadaic acid, Campàs et al.[22] have reported the selection of an aptamer targeting OA and its use in the development of competitive colorimetric assay. However, the aptamer sequence and the detection results have not been published so far. An ongoing work and submitted patent by another research group has been recently referred to.[23] However, no results have been published yet. Here we report for the first time the selection, identification, characterization, and biosensing application of a high-affinity aptamer for okadaic acid. The aptamer has been selected using systematic evolution of ligand by exponential enrichment (SELEX) and successfully applied in designing a label-free aptasensor for okadaic acid detection.

EXPERIMENTAL SECTION

Materials and Reagents. The DNA library and primers for polymerase chain reaction (PCR) were custom-synthesized by Integrated DNA Technologies Inc. (Coralville, U.S.A.). The 5′-C_6 disulfide terminated aptamer (5′HO−$(CH_2)_6$−S−S−$(CH_2)_6$/GGTCACCAAC AACAGGGAGC GCTACGCGAA GGGTCAATGT GACGTCATGC GGATGTGTGG/-3′) was synthesized by GenScript (New Jersey, U.S.A.). Diaminodipropylamine agarose (DADPA) beads and 1-ethyl-3-(3-dimethylaminopropyl) carbodiimide hydrochloride (EDC) were obtained from Fisher Scientific (Ontario, Canada). Sodium carbonate anhydrous, sodium bicarbonate, sodium azide, Taq plus DNA polymerase, acrylamide/bisacrylamide (40% solution), urea, Tris-base, boric acid, EDTA disodium dihydrate, and ethanol were purchased from Bioshop Inc. (Ontario, Canada). Okadaic acid sodium salt and microcystin-LR were purchased from Enzo Life Sciences (Ontario, Canada). DTX-1 and DTX-2 were purchased from National Research Council Canada−Institute for Marine Biosciences (Halifax, Canada). Monoclonal antibody (anti-OA-mAb, developed in mouse) against OA was obtained from Abcam (Cambridge, U.S.A.). TOPO TA cloning kit with One Shot MAX Efficiency DH5α-T1, 3,3′,5,5′-tetramethylbenzidine (TMB) stabilized chromogen and HRP-labeled goat antimouse IgG antibodies were purchased from Invitrogen (New York, U.S.A.). Potassium ferrocyanide ($K_4Fe(CN)_6$), potassium ferricyanide ($K_3Fe(CN)_6$), dipotassium hydrogen orthophosphate, potassium dihydrogen orthophosphate, sodium chloride, 2-(*N*-morpholino)ethanesulfonic acid (MES), bovine serum albumin (BSA), and magnesium chloride were purchased from Sigma (Ontario, Canada). Amicon Ultra-0.5 mL centrifugal desalting filters with a 3 kDa molecular cutoff were obtained from EMD Millipore (Alberta, Canada). Centrifuge tube filters with a cellulose acetate membrane with pore size of 0.45 μm were purchased from Corning life sciences (Tewksbury MA, U.S.A.). Binding buffer was used during the aptamer selection as well as the electrochemical experiments which consist of 50 mM Tris, pH 7.5, 150 mM NaCl, 2 mM $MgCl_2$. Elution buffer is 7 M urea in binding buffer. Tris−EDTA buffer (TE buffer) is 10 mM Tris, pH 7.4, 1 mM EDTA. A phosphate-buffered saline PBS solution (10 mM, pH 7.4) was used for the preparation of the antibody and washing of the okadaic acid beads in the ELISA experiments. MES buffer, 0.9% NaCl, pH 4.7 was used for coupling of okadaic acid with the DADPA beads. All solutions were prepared using Milli-Q grade water.

Instrumentation. Electrochemical experiments were carried out using a model 660D potentiostat/galvonastat (CH Instruments Inc. U.S.A.), controlled by a personal computer via a CH Instruments software. A three-electrode system was used for all the electrochemical measurements, consisting of a gold working electrode, a Ag/AgCl electrode as the reference, and a Pt wire as the auxiliary electrode. The UV and fluorescence measurements were performed using NanoDrop 2000C spectrophotometer and NanoDrop 3300 fluorospectrometer, respectively (Fisher Scientific, Canada). Circular dichroism (CD) measurements were done using Jasco-810 spectropolarimeter.

Methods. *Coupling of Okadaic Acid to Agarose Beads.* An amount of 100 μg of okadaic acid was first dissolved in 100 μL of methanol and then diluted to 1 mL with coupling buffer. A volume of 2 mL of DADPA beads was washed several times with coupling buffer. An amount of 30 mg of EDC was dissolved in 0.5 mL of coupling buffer and mixed with the okadaic acid solution. Then, the mixture was immediately added to washed agarose beads and the final volume was made up to 4 mL with coupling buffer. The mixture was rotated for 3 h at room temperature. After the reaction, the beads were washed with 1 M NaCl solution in order to remove the excess unreacted toxin. Then, the beads were equilibrated with 0.2 M carbonate buffer, pH 8.5, and 20 mg of sulfo-NHS acetate was added in order to quench the unreacted amine groups on the beads. The mixture was rotated for another hour, after which the beads were washed extensively with binding buffer (50 mM Tris, pH 7.5, 150 mM NaCl, 2 mM $MgCl_2$). The DTX-1 and DTX-2 beads were also prepared following the same protocol. The success of the immobilization of OA, DTX-1, and DTX-2 on the beads was confirmed by direct ELISA using the toxin-conjugated beads and free beads as a control. ELISA was performed by incubating the beads with anti-OA-mAb (diluted 1:1000 in PBS buffer pH 7.4) for 1 h after washing with PBS buffer and blocking with 1% BSA solution. Then the beads were washed again, and a secondary antibody was added and incubated for another 1 h. After washing and incubating the beads for 15 min with stabilized chromogen (TMB) solution, a blue color was produced in the toxin-coated beads; while no color was observed when the free beads were used which confirms the success of the coupling reaction. During the

dx.doi.org/10.1021/ac402220k | *Anal. Chem.* XXXX, XXX, XXX−XXX

SELEX rounds, the ELISA experiments for OA-coated beads were repeated several times to eliminate the possibility of OA leaching from the beads during the storage, and all the experiments confirmed the presence of okadaic acid and the stability of the beads. Simultaneously, negative beads were prepared for the counter selection round by adding 40 mg of sulfo-NHS acetate to 500 μL of DADPA beads equilibrated in carbonate buffer, pH 8.5. Finally, the positive OA beads and the negative beads were stored in binding buffer containing 0.02% sodium azide at 4 °C until use.

In Vitro Selection of the DNA Aptamer. The library and the primer sets were designed according to a protocol reported previously.[24] A random ssDNA library (10^{15} oligonucleotides) was used which consisted of a central random region of 60 nucleotides flanked by two fixed regions of 18 nucleotides-sequences at the 3′ and 5′ ends. These regions represent the primer binding sites for the amplification (5′-ATACCAGCTT-ATTCAATT-N_{60}-AGATAGTAAGTGCAATCT-3′). An amount of 100 μL of OA beads was washed several times with binding buffer. Amounts (3 nmol at the first selection round and 150 pmol in the subsequent rounds) of ssDNA pool were heated to 90 °C for 5 min, cooled at 4 °C for 10 min, kept at 25 °C for 5 min, and then added to the washed OA beads in 300 μL binding buffer in a centrifuge filter tube. The mixture was incubated at room temperature with end-over-end rotation for 2 h. The beads were then washed with binding buffer. Then, the DNA bound to OA beads was eluted with 400 μL aliquots of elution buffer for six times with heating at 90 °C for 10 min until no DNA is detected. The eluted DNA was desalted and concentrated by an ultrafiltration device. In a counter selection round, the DNA pool was first incubated with the negative beads; washed DNA was collected, subjected to the same heating and cooling treatment, and subsequently incubated with OA beads. The selected DNA pools were amplified by PCR in 15 parallel 75 μL reactions each containing 2 units of Taq Plus and polymerase buffer, 2 mM $MgCl_2$, 200 μM dNTP, and 0.2 μM of forward and reverse primers. The primers were designed and modified with fluorescein and a PEG linker followed by a poly-A tail as reported previously.[24,25] Forward primer was 5′-fluorescein-ATACCAGCTTATTCAATT-3′; reverse primer was 5′-poly(dA_{20})-PEG_6-AGATTGCACT-TACTATCT-3′. PCR conditions were as follows: 94 °C for 10 min, followed by 25 cycles of 94 °C for 1 min, 47 °C for 1 min, 72 °C for 1 min, and a final extension step of 10 min at 72 °C. PCR products were dried by a SpeedVac, resuspended in 50:50 water and formamide and heated to 55 °C for 5 min. The relevant DNA strand (labeled with fluorescein) was separated from the double-stranded PCR product in 12% denaturing PAGE and eluted from the gel band by freeze−thaw cycle. Eluted ssDNA in TE buffer was concentrated, desalted by ultrafiltration, quantified by UV, and used for the next selection round.

Cloning and Sequencing of Selected DNA. After 18 selection rounds where DNA recoveries began to plateau, the selected ssDNA was amplified with the nonmodified primer set and cloned into pCR2.1-TOPO vector using the TOPO TA cloning kit. Colonies were grown on LB-agar medium supplemented with ampicillin, X-Gal, and IPTG. Positive colonies were picked and grown in liquid media. ssDNA inserts were PCR-amplified using the M13 forward and reverse primer sites within the vector and sequenced. Sequences of the selected ssDNAs were analyzed and aligned using PRALINE.[26]

Dissociation Constants Determination by Fluorescence Assay. The selected aptamers sequences were amplified by PCR with the labeled primers used during the selection rounds, and the fluorescein-labeled sequences were separated by gel electrophoresis as described above. Different concentrations of each sequence (0−300 nM) in binding buffer were incubated with 20 μL of OA beads in a centrifuge tube after being subjected to the heating and cooling treatment as described above in the selection step. The fluorescence of the eluted DNA from each sample was measured, and the saturation curve was obtained. The dissociation constant (K_d) for each sequence with OA was calculated by nonlinear regression analysis.

Analysis of the Conformation Change of the Aptamer Using Circular Dichroism. Circular dichroism spectroscopy was used to examine the conformational change in the aptamer (OA32) with OA. The assay was performed using solutions of DNA aptamer: 0.67 μM with 0.67 μM OA in a 1 cm path length, quartz cuvette in an optical chamber. The chamber was deoxygenated with dry purified nitrogen (99.99%) before use and kept in the nitrogen atmosphere during experiments. Each CD spectrum was collected from 230 to 340 nm at 0.1 nm intervals, the accumulation of three scans at 20 nm/min, with a 1 nm bandwidth and a time constant of 1 s.

Preparation of the Aptamer-Modified Electrodes. Prior to modification, the gold electrodes (2 mm in diameter) were polished with alumina slurry (Al_2O_3) of various particle sizes (1.0, 0.3, and 0.05 μm), followed by washing with Milli-Q water, ultrasonication for 5 min, and drying in a nitrogen stream. The electrodes were then cleaned in piranha solution (3:1 mixture of concentrated H_2SO_4 and 30% H_2O_2 for 10 min) and washed with Milli-Q water. Next, the electrodes were electrochemically cleaned in 0.1 M H_2SO_4 by cyclic voltammetry scanning between 0.0 and 1.6 V for 5 min, followed by washing with ultrapure water and drying under nitrogen. Then, the aptamer sequence with the highest affinity to OA was immobilized on the gold electrodes by immersion in 1 μM solution of the 5′-disulfide terminated aptamer in binding buffer for 24 h. After modification, the electrodes were rinsed with binding buffer solution, followed by incubation in 1 mM 6-mercapto-1-hexanol (MCH) in 10 mM phosphate buffer, pH 7.0 for 30 min. The modified electrodes were then washed thoroughly with binding buffer and immediately used in the electrochemical experiments, or kept in binding buffer solution at 4 °C until further use.

Electrochemical Measurements. For the okadaic acid detection, specificity and cross-reactivity experiments, a 5 μL droplet of OA, MC-LR, DTX-1, or DTX-2 in binding buffer was added onto the aptamer-modified gold electrodes surface and incubated for 30 min. The electrodes were then washed with binding buffer to remove the nonspecifically bound toxins and subjected to electrochemical measurements. The CV experiments were conducted at a scan rate of 100 mV/s. The electrochemical impedance spectroscopy (EIS) measurements were recorded over a frequency range from 10 kHz to 0.1 Hz using an alternative voltage with an amplitude of 10 mV, superimposed on a dc potential of 0.23 V (vs a Ag/AgCl reference electrode). The impedance data were plotted in the form of a complex plane diagram (Nyquist plot) with a sampling rate of 25 points per decade. The obtained spectra were fitted using the CH Instruments fitting program. All the EIS and CV measurements were recorded in a 0.1 M PBS buffer solution containing 5 mM $[Fe(CN)_6]^{3-/4-}$ redox pair (1:1 molar ratio).

dx.doi.org/10.1021/ac402220k | Anal. Chem. XXXX, XXX, XXX−XXX

Table 1. Sequences and Dissociation Constants (K_d) between OA and Selected Aptamers

group	clone no.	aptamer sequence	K_d (nM)
A	OA 24	GGCGGACCAAGGGGACACCACAGATGAATGTACAGTACCATGTTACTGCGCCCGTAGGTG	126
B	OA 21	GGGGCAACAAACACGGAAGAAAATGAATCTACATACGTGGACATATATCCTGCCGCGTG	983
C	OA 34	GGTCACCAACAACAGGGAGCGCTACGCGAAGGGTCAATGTGACGTCATGCGGATGTGTGG	77
D	OA 18	GGCCGCGAGAGAGACAACAAGGATATATATTATATGTCGGTTGTAGTGTTGGGTTGCG	–
E	OA 11	GGGACAGCGGAGGTCTCCCACCCACCGGCCCCTGCGGCACACCAACCTGTATGGATGCG	131
F	OA 32	GCCATGACAACCAGAGGTACCCCCGCCCACCAGCCCCGAAGTCTGTCAGCCTAGTTGTTG	380
G	OA 6	GGCCACCAACGAGAGTCAGAAAACCATGGTGGGTATACCAGGAGGTCCATGCGTGCTGTG	–
H	OA 22	CCACACAACAGCCTACGTGGATACACCACATACATCCCATAACCCCGTGTCATGTGTCG	183

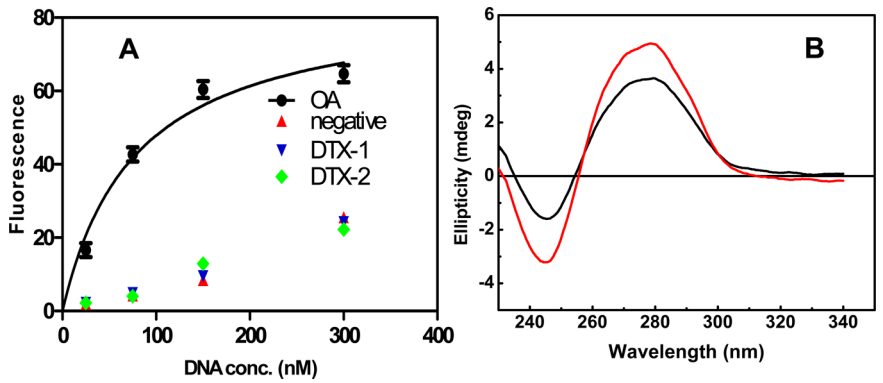

Figure 1. (A) Fluorescence binding assay of aptamer OA34 with OA beads (black curve), negative (red curve), DTX-1 (blue curve), and DTX-2 beads (green curve). The K_d of OA−aptamer was determined to be 77 nM. Each point is the mean of three experiments, and error bars represent the standard deviations of the measurements. (B) Circular dichroism spectra of 0.67 μM aptamer OA34 in binding buffer before (black) and after (red) binding with 0.67 μM of OA at room temperature.

Scheme 1. Fabrication of the Impedimetric Aptasensor Based on Label-Free Target-Induced Folding of the Aptamer

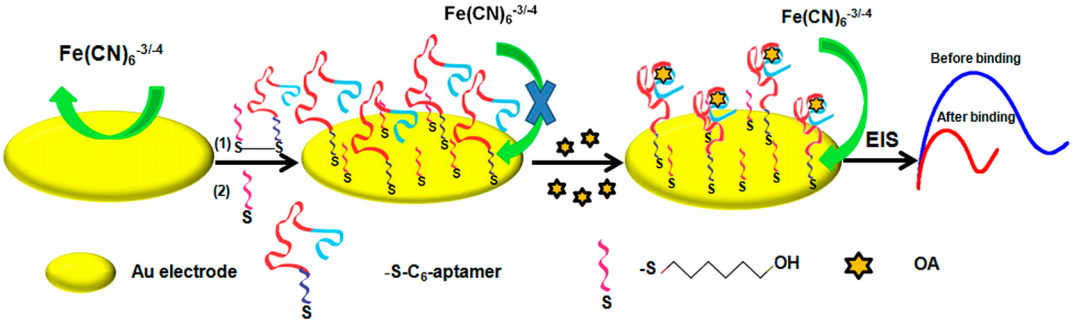

RESULTS AND DISCUSSION

Okadaic Acid Aptamer Selection. We immobilized OA on DADPA agarose beads by coupling the terminal carboxylic groups on the toxin with the amine groups on the beads via EDC/NHS chemistry. This design keeps the rest of the functional groups on the OA molecule accessible for DNA binding during the selection. The remaining free amino groups on the beads were blocked with sulfo-NHS acetate in order to reduce the nonspecific binding of the beads with the DNA.[19] A DNA library consisting of 10^{15} random 60-nucleotide sequences was screened against OA beads in a SELEX procedure. A counter selection was performed after the fourth round to eliminate the DNA sequences which bind to the agarose beads. After 18 rounds of selection, when significant enrichment of okadaic acid binding DNA was observed (Supporting Information Figure S2), the selection cycles were stopped and the eluted DNA from the last round was cloned. We randomly selected 42 clones for sequencing, and the identified sequences were analyzed by multiple sequence alignment using the PRALINE software[26] and then grouped into eight families based on their similarities. Significant consensus regions between the sequences in each group were observed, and some sequences were identical (Supporting Information Figure S3). Therefore, one sequence from each group was randomly chosen for further binding affinity studies with OA as shown in Table 1. Binding assays using a constant amount of OA beads and different concentrations of fluorescein-labeled aptamers (0−300 nM) were performed using the same SELEX conditions. The beads were washed several times, and the bound aptamers were eluted. The fluorescence of the eluted aptamers was then measured and plotted versus the aptamer concentration used for binding. The dissociation constants (K_d) of the selected aptamers were calculated by nonlinear regression analysis; Figure 1A is an example of OA34 sequence. Six aptamers have shown good affinity to OA ranging from 77 to 980 nM, and two aptamers did not exhibit binding. The highest affinity to OA was obtained for aptamer (OA34) with a K_d of 77 nM and therefore

dx.doi.org/10.1021/ac402220k | Anal. Chem. XXXX, XXX, XXX−XXX

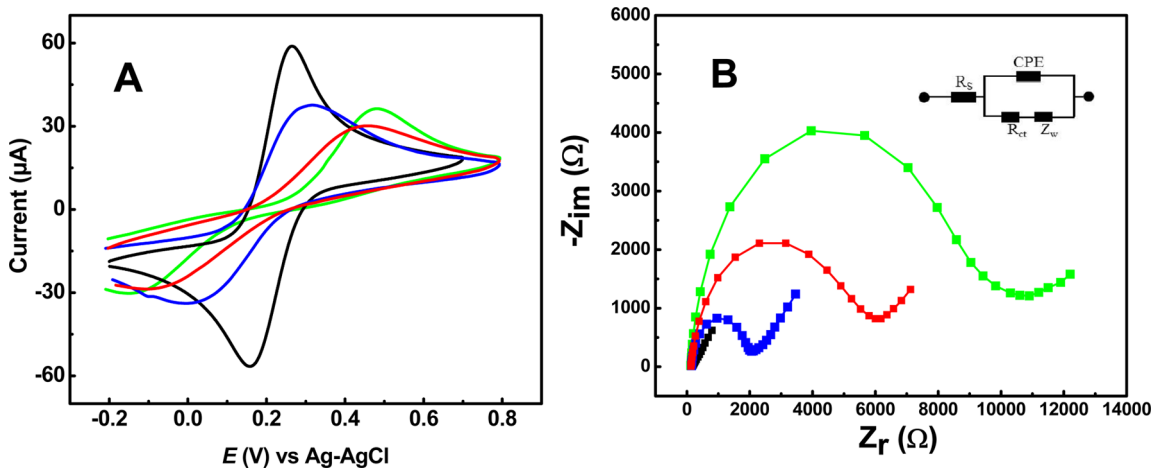

Figure 2. Cyclic voltammetry (A) and Nyquist plots (B) of 5 mM $[Fe(CN)_6]^{4-/3-}$ redox couple in PBS, pH 7.4, for bare Au electrode (black), Au/aptamer (red), Au/aptamer/MCH (green), and after binding with 60 ng/mL OA (blue). The cyclic voltammetry was performed at a scan rate of 100 mV/s, and the EIS was performed using a frequency range of 10^4 to 0.1 Hz, a dc potential of +0.23 V, and ac amplitude of 5 mV. The inset in panel B is the equivalent circuit applied to fit the impedance spectra.

was used for further experiments. The binding of OA34 was tested with the negative agarose beads, and the cross-reactivity with DTX-1 and DTX2 beads was also assessed. As shown in Figure 1A, OA34 did not exhibit binding to both negative, DTX-1. and DTX-2 beads. These results indicate the high selectivity of OA34 against DTX-1 and DTX-2, toxins closely related to OA differing only by two methyl groups. We then used circular dichroism in order to gain insight on the conformation of the free and target-bound form of OA34. As shown in Figure 1B, before the addition of OA into the solution containing aptamer, the circular dichroism spectrum of the aptamer showed a positive band at 277 nm and a negative band at about 245 nm. Upon OA binding, an increase of the ellipticity at 277 and 245 nm was observed. This change in the CD spectra indicates the folding of the aptamer into a different conformation upon binding with OA.

Impedimetric Aptasensor for OA Detection. The aptamer with the highest affinity to OA (OA34) was then used to fabricate a label-free aptasensor based on EIS detection. EIS is a powerful, nondestructive technique able to monitor the change of the interfacial properties at the electrode surface upon any modification.[10] As shown in Scheme 1, the aptasensor was constructed using a self-assembled monolayer (SAM) of disulfide-modified aptamer on a polycrystalline gold electrode. Then the aptamer-modified electrodes were blocked by MCH in order to minimize the nonspecific adsorption of the aptamers on the gold surface which could affect the efficiency of the sensor.[27−30] The detection mechanism of the aptasensor is based on probing the change in the impedimetric signal caused by the change of the aptamer conformation upon aptamer−toxin binding.

The characterization of the aptasensor fabrication steps was performed using CV and EIS. Figure 2A shows the cyclic voltammograms of the bare Au, Au/aptamer, Au/aptamer/MCH, and after binding with 60 ng/mL OA in 5 mM solution of $[Fe(CN)_6]^{4-/3-}$ couple in PBS buffer. The $[Fe(CN)_6]^{4-/3-}$ redox probe exhibited a characteristic reversible behavior on the bare gold electrode (Figure 2A, black curve) with a peak-to-peak separation of almost 80 mV, indicating a clean gold surface. After the immobilization of the aptamer (Figure 2A, red curve) the peak-to-peak separation increased, and a substantial decrease in the peak current was also observed. This change is due to the negative charge on the DNA aptamer which repels the negatively charged $[Fe(CN)_6]^{4-/3-}$ anions, retarding the electron transfer between the redox probe and the electrode surface. Then, a further increase in the peak-to-peak separation was observed after blocking the electrodes with MCH (Figure 2A, green curve) indicating an additional decrease of the electron-transfer rate due to the filling of some empty spaces on the gold surface. However, after the incubation of the aptasensor in 60 ng/mL OA, the redox peaks current increased and the peak-to-peak separation was decreased (Figure 2A, blue curve). This result suggests a conformation change within the aptamer upon binding with OA, thereby favoring the access of the $[Fe(CN)_6]^{3-/4-}$ redox couple to the sensor surface.

Figure 2B shows the Nyquist plots for the bare Au, Au/aptamer, and Au/aptamer/MCH and after binding with OA. Each spectrum is composed of a semicircular part in a high-frequency region and a linear part in a low-frequency region, corresponding to the electron-transfer process and the diffusion process, respectively. The impedance spectra were fitted by a modified Randles equivalent circuit (shown in the inset of Figure 2B) consisting of the solution resistance (R_s), charge-transfer resistance (R_{ct}), constant phase element (CPE), and Warburg impedance (Z_w).[31,32] The diameter of the semicircle corresponds to the charge-transfer resistance. The bare gold electrode shows a characteristic very small semicircle domain which indicates very fast electron-transfer process with a diffusion-limiting step (Figure 2B, black curve). The self-assembly of the negatively charged aptamer on the electrode surface significantly increase the diameter (Figure 2B, red curve) of the semicircle which indicates an increase in the charge-transfer resistance due to the repulsion of the aptamer on the electrode surface with the $[Fe(CN)_6]^{4-/3-}$ anions. After the incubation with MCH the R_{ct} was further increased due to the filling of some of the exposed gold areas which introduces a barrier to the interfacial electron transfer (Figure 2B, green curve). After okadaic acid binding, a large drop in R_{ct} was observed (Figure 2B, blue curve). This decrease in the R_{ct} is consistent with the CV behavior explained above and is likely due to the conformational change of the aptamer upon binding with the toxin to a more compact structure. The decrease of the

dx.doi.org/10.1021/ac402220k | Anal. Chem. XXXX, XXX, XXX−XXX

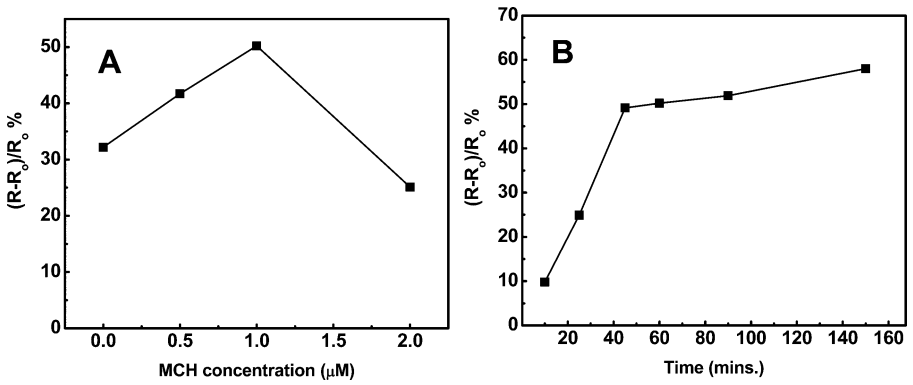

Figure 3. (A) Effect of MCH concentration and (B) the effect of the OA incubation time on aptasensor response toward 30 ng/mL OA in 10 mM PBS (pH 7.4) containing 5 mM $[Fe(CN)_6]^{4-/3-}$ redox couple.

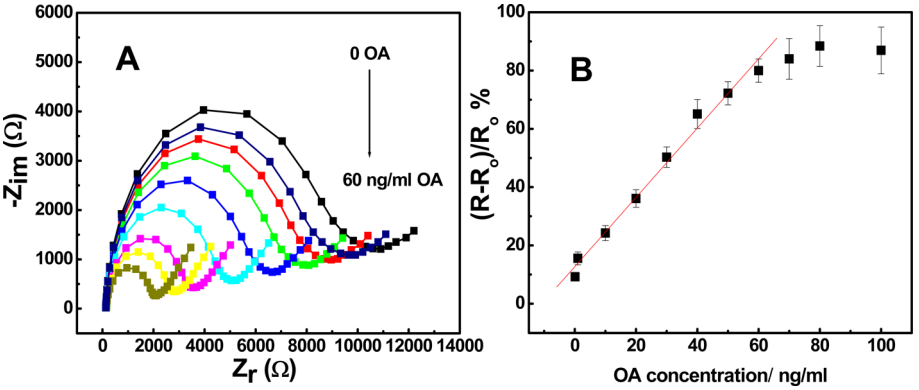

Figure 4. (A) Nyquist plots of the aptasensor after incubation with different concentrations of OA 0.00, 0.1, 1.0, 10, 20, 30, 40, 50, and 60 ng/mL. (B). The calibration curve for OA, plot of $\Delta R_{ct}/R_o\%$ vs C_{OA}. The error bars show the standard deviation of three repetitive measurements.

R_{ct} induced by aptamer−target binding has been previously observed elsewhere.[33,35,36]

It is well-established that the addition of MCH to form a mixed monolayer with thiol-modified DNA is an essential step to control the film formation process and preserve the conformation of the surface-anchored DNA oligonucleotides.[37] Here, we utilized an $5'HO-(CH_2)_6-S-S-(CH_2)_6$ modified aptamer to coimmobilize self-assembled monolayer of the OA aptamer and MCH, where the disulfide bond would break upon chemisorption and a mixed SAM would form. With the aim of studying the effect of adding extra MCH on the sensor response, a treatment of the aptamer−MCH modified electrodes was carried out with different concentrations of extra MCH. Figure 3A shows the different responses of the aptasensors blocked with different concentrations of MCH after incubation with 30 ng/mL OA solution. The aptasensor response quantified as $((R_o - R)/R_o\ \%)$ increased by the addition of extra MCH from 0 to 1 μM. These results indicate that the coimmobilization process was not enough to remove the physisorbed DNA on the gold surface or to retain the conformation of the surface-attached DNA which affects the binding with OA. We found that, when the electrodes were incubated with an extra 1 μM concentration of MCH, the binding and, consequently the sensor response, was significantly improved. However, adding even higher concentration of MCH caused the aptasensor response to decrease again which could be due to the blocking of most of the pinholes on the gold surface. This higher coverage of the gold surface decreased the electron-transfer rate, and subsequently the change in the resistance upon target binding was decreased. Therefore, 1 μM of extra MCH was chosen for blocking the electrodes in the subsequent experiments.

Since the assay time is a very important factor for biosensor's performance and their practical application, it was also crucial to optimize the incubation time of OA on the aptasensor. The aptasensor's response was monitored after incubating 30 ng/mL OA on the aptasensor at different time points. Figure 3 shows a significant difference in R_{ct} as sensor response with increasing incubation time. The maximum response $((R_o - R)/R_o\ \%)$ was observed after 45 min incubation, after which a very small increase in response signal was observed. Therefore, 45 min was chosen as the optimum binding time in the following experiments.

We then studied the aptasensor impedimetric response toward okadaic acid concentrations in the range of 100 pg/mL to 100 ng/mL. As shown in Figure 4A, marked drops in the diameter of the semicircle were observed with increasing concentrations of OA due to conformation change of the aptamer molecules upon binding with OA as explained above. A calibration plot based on the percentage change in the R_{ct} after the OA binding is shown in Figure 4B. The data points in the calibration curve represent three independent measurements, and the error bars show the standard deviations ranging from 1.0% to 7.0%, indicating good reproducibility of the aptasensor response. A good linear relationship was obtained in the concentration range from 100 pg/mL to 60 ng/mL which can be represented by the linear regression equation $(R_o - R)/R_o\ \% = 12.75 + 1.19C\ [\text{ng mL}^{-1}]$, $R = 0.994$, with a detection limit (LOD) of 70 pg/mL. The limit of detection (LOD) was calculated from $3(S_b/m)$, where S_b is the standard deviation of

dx.doi.org/10.1021/ac402220k | Anal. Chem. XXXX, XXX, XXX−XXX

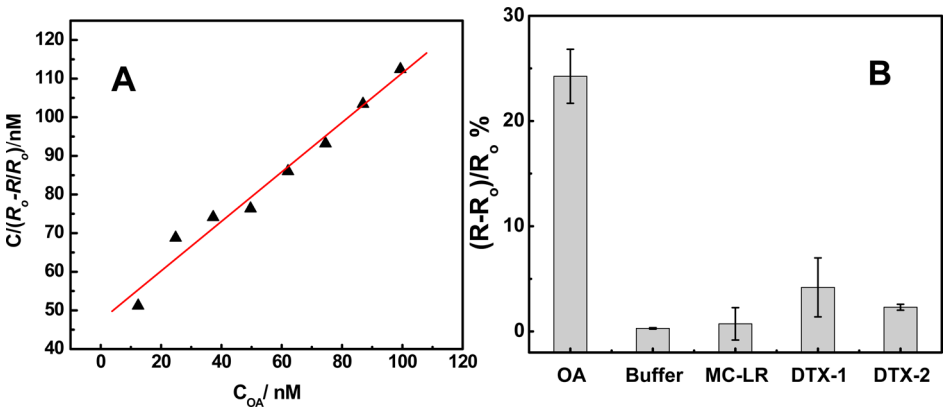

Figure 5. (A) Linearized adsorption isotherm of OA binding to its aptamer immobilized on gold electrode based on the Langmuir model. The line is the best linear fit to the experimental data from which the dissociation constant (K_d) was determined. (B) Comparison of the response of the aptasensor after incubation with 10 ng mL^{-1} OA, binding buffer, MC-LR, DTX-1, and DTX-2.

the measurement signals for the blank and m is the slope of the analytical curve. This detection limit is lower than the detection limit of the available commercial ELISA kit as well as than other reported immunosensors[11,13]

In order to understand the effect of the gold surface immobilization of the aptamer on its binding affinity with OA, we calculated the dissociation constant of OA−aptamer using EIS. The calculations are based on the classical Langmuir isotherm,[1] which assumes equal binding energy for all binding sites on the surface and that the ability of the molecule to bind is independent of whether adjacent sites are filled. The equilibrium of OA and its aptamer (AP) binding can be represented as follows:

$$[\mathrm{AP{-}OA}] \rightleftharpoons [\mathrm{AP}] + [\mathrm{OA}]$$

so the $K_d = ([\mathrm{AP}][\mathrm{OA}])/[\mathrm{AP{-}OA}]$. Assuming that the surface coverage of the aptamer−OA complex [AP−OA] is θ, the surface coverage of unbound aptamer [AP] will be $(1 - \theta)$, so $K_d = (1 - \theta)[\mathrm{OA}]/\theta$.

On the basis of the Langmuir model, we assume that the change of R_{ct} is directly related to the OA−aptamer binding according to the equation:

$$\Delta R = \theta\ \Delta R_{sat}$$

where $\Delta R = (R_o - R)/R_o$ and ΔR_{sat} is the maximum aptasensor response $(R_o - R_{sat})/R_o$. A linearized form of the Langmuir isotherm can be represented by the following equation:[34−38]

$$\frac{C_{OA}}{\Delta R} = \frac{C_{OA}}{(\Delta R)_{sat}} + \frac{K_d}{(\Delta R)_{sat}}$$

By plotting $C_{OA}/\Delta R$ as a function of the molar concentration of OA (C_{OA}) (Figure 5A) while avoiding the responses from low OA concentrations, K_d can be obtained by dividing the y-intercept by the slope. Using this method we obtained a K_d of 74 ± 6.2 nM, which is in very good agreement with the value obtained by the fluorescence assay in solution. This result indicates that the binding affinity of the aptamer with OA was not affected by the disulfide modification and the subsequent immobilization on the gold surface.

A preliminary application of the proposed OA aptasensor in real samples was examined by performing measurements for spiked uncontaminated shellfish extracts. The extraction was done following the protocol reported previously, and then the samples were spiked with 10 ng/mL OA. The recovery percent calculated using the calibration curve performed in binding buffer was about 92% demonstrating possible applicability of the aptasensor in real samples.

Negative control experiments using MC-LR and assessment of cross-reactivity to DTX-1 and DTX-2 were also performed using 10 ng/mL of each toxin. As shown in Figure 5B, no significant response (change in the R_{ct}) was obtained with all the nontargeted toxins. In particular, the aptasensor did not exhibit cross-reactivity to DTX-1 and DTX-2. These results confirm that the developed aptasensor is very selective to OA. We believe that the continual selection of high-selectivity aptamers against other analogues and their integration in a single biosensor device will facilitate routine monitoring of the OA group of toxins with more accurate estimate of toxicity.

CONCLUSION

This work shows the first selection, identification, and biosensing application of DNA aptamers for the marine toxin okadaic acid. The highest affinity aptamer (K_d = 77 nM) showed remarkable sensitivity and selectivity for OA against DTX-1 and DTX-2. We showed that the affinity of the aptamer toward OA was preserved and not affected by surface immobilization. The circular dichroism spectra also demonstrated the conformation change of the aptamer upon OA binding which can be exploited in several biosensing applications. Through monitoring of the OA binding induced conformational change within the aptamer, we achieved a limit of detection of 70 pg/mL with a label-free aptasensor based on electrochemical impedance spectroscopy. We believe that the continual emergence of novel library-selected, high-affinity aptamers will open the way to a variety of biosensing architectures, particularly for sensitive and high-specificity small-molecule toxin detection in complex samples.

ASSOCIATED CONTENT

Supporting Information

Additional information as noted in text. This material is available free of charge via the Internet at http://pubs.acs.org.

AUTHOR INFORMATION

Corresponding Author

*E-mail: m.zourob@cranfield.ac.uk. Phone: +44 0 1234 758318.

dx.doi.org/10.1021/ac402220k | *Anal. Chem.* XXXX, XXX, XXX−XXX

Notes

The authors declare no competing financial interest.

■ ACKNOWLEDGMENTS

The authors extend a special gratitude to NSERC for funding. The authors also acknowledge Dr. Raja Chinnappan for his help and fruitful discussions about SELEX experiments and Dr. Steve Bourgault, for the help in performing the CD spectrometry measurements.

■ REFERENCES

(1) Steidinger, K. A. *Algal Toxins in Seafood and Drinking Water*; Academic Press: New York, 1993.
(2) Morton, S. L.; Tindall, D. R. *Toxicon* **1996**, *34*, 947−954.
(3) Dounay, A. B.; Forsyth, C. J. *Curr. Med. Chem.* **2002**, *9*, 1939−1980.
(4) Mestrovic, V.; Pavela Vrancic, A. *Biochimie* **2003**, *85*, 647−650.
(5) Suganuma, M.; Fujuki, H.; Suguri, H.; Yoshizawa, S.; Hirota, M.; Nakayasu, M.; Ojika, M.; Wakamatsu, K.; Yamada, K.; Sugimura, T. *Proc. Natl. Acad. Sci. U.S.A.* **1988**, *85*, 1768−1773.
(6) Yasumoto, T.; Oshima, Y.; Yamaguchi, M. *Bull. Jpn. Soc. Fish.* **1978**, *44*, 1249−1255.
(7) Hayat, A.; Barthelmebs, L.; Sassolas, A.; Marty, J.-L. *Talanta* **2011**, *85*, 513−518.
(8) Marquette, C. A.; Coulet, P. R.; Blum, L. J. *Anal. Chim. Acta* **1999**, *398*, 173−182.
(9) Prieto-Simón, B.; Miyachi, H.; Karube, I.; Saiki, H. *Biosens. Bioelectron.* **2010**, *25*, 1395−1401.
(10) Vaughan, R. D.; Geary, E.; Pravda, M.; Guilbault, G. G. *Int. J. Environ. Anal. Chem.* **2003**, *83*, 555−571.
(11) Tang, A. X. J.; Pravda, M.; Guilbault, G. G.; Piletsky, S.; Turner, A. P. F. *Anal. Chim. Acta* **2002**, *471*, 33−40.
(12) Campàs, M.; de la Iglesia, P.; Le Berre, M.; Kane, M.; Diogène, J.; Marty, J.-L. *Biosens. Bioelectron.* **2008**, *24*, 716−722.
(13) Hayat, A.; Barthelmebs, L.; Marty, J.-L. *Anal. Chim. Acta* **2011**, *690*, 248−252.
(14) Eissa, S.; Zourob, M. *Nanoscale* **2012**, *4*, 7593−7599.
(15) Tuerk, C.; Gold, L. *Science* **1990**, *249*, 505−510.
(16) Ellington, A. D.; Szostak, J. W. *Nature* **1990**, *346*, 818−822.
(17) Bunka, D. H. J.; Stockley, P. G. *Nat. Rev. Microbiol.* **2006**, *4*, 588−596.
(18) Sefah, K.; Phillips, J. A.; Xiong, X.; Meng, L.; Van Simaeys, D.; Chen, H.; Martin, J.; Tan, W. *Analyst* **2009**, *134*, 1765−1775.
(19) Cruz-Aguado, J. A.; Penner, G. *J. Agric. Food Chem.* **2008**, *56*, 10456−10461.
(20) McKeague, M.; Bradley, C. R.; De Girolam, A.; Visconti, A.; Miller, J. D.; DeRosa, M. C. *Int. J. Mol. Sci.* **2010**, *11*, 4864−4881.
(21) Handy, S. M.; Yakes, B. J.; DeGrasse, J. A.; Campbell, K.; Elliott, C. T.; Kanyuck, K. M.; DeGrasse, S. L. *Toxicon* **2013**, *61*, 30−37.
(22) Campàs, M.; Reverté, L.; Freixes, G.; de la Iglesia, P.; Diogène, J.; Prieto-Simón, B. Presented at the *2nd International Conference on Bio-Sensing Technology*, Amsterdam, The Netherlands, October 10−12, 2011; P131.
(23) Sassolas, A.; Hayat, A.; Catanante, G.; Marty, J. L. *Talanta* **2013**, *105*, 306−316.
(24) Ng, A.; Chinnappan, R.; Eissa, S.; Liu, H.; Tlili, C.; Zourob, M. *Environ. Sci. Technol.* **2012**, *46*, 10697−10703.
(25) Stoltenburg, R.; Reinemann, C.; Strehlitz, B. *Anal. Bioanal. Chem.* **2005**, *383*, 83−91.
(26) Simossis, V. A.; Kleinjung, J.; Heringa. *Nucleic Acids Res.* **2005**, *33*, 816−824.
(27) Xiao, Y.; Piorek, B. D.; Plaxco, K. W.; Heeger, A. J. *J. Am. Chem. Soc.* **2005**, *127*, 17990−17991.
(28) Steel, A. B.; Herne, T. M.; Tarlov, M. J. *Anal. Chem.* **1998**, *70*, 4670−4677.
(29) Liu, Y.; Tuleouva, N.; Ramanculov, E.; Revzin, A. *Anal. Chem.* **2010**, *82*, 8131−8136.
(30) White, R. J.; Phares, N.; Lubin, A. A.; Xiao, Y.; Plaxco, K. W. *Langmuir* **2008**, *24*, 10513−10518.
(31) Randles, J. *Discuss. Faraday Soc.* **1947**, *1*, 11−20.
(32) Bard, A. J.; Faulkner, L. R. *Electrochemical Methods: Fundamentals and Applications*, 2nd ed.; Wiley & Sons: New York, 2001.
(33) Kashefi-Kheyrabadi, L.; Mehrgardi, M. A. *Biosens. Bioelectron.* **2012**, *33*, 184−189.
(34) Cheng, A. K. H.; Ge, B.; Yu, H.-Z. *Anal. Chem.* **2007**, *79*, 5158−5164.
(35) Lin, Z.; Huang, H.; Xu, Y.; Gao, X.; Qiu, B.; Chen, X.; Chen, G. *Talanta* **2013**, *103*, 371−374.
(36) Labib, M.; Zamay, A. S.; Muharemagic, D.; Chechik, A. V.; Bell, J. C.; Berezovski, M. V. *Anal. Chem.* **2012**, *84*, 1813−1816.
(37) Lao, R.; Song, S.; Wu, H.; Wang, L.; Zhang, Z.; He, L.; Fan, C. H. *Anal. Chem.* **2005**, *77*, 6475−6480.
(38) Huang, Y.; Bell, M. C.; Suni, I. I. *Anal. Chem.* **2008**, *80*, 9157−9161.